Journal of Industrial and Engineering Chemistry xxx (xxxx) xxx

Contents lists available at ScienceDirect

Journal of Industrial and Engineering Chemistry

journal homepage: www.elsevier.com/locate/jiec

Full Length Article

Enhanced copper-adsorption removal from water by easy-handling silica aerogel-polyurethane foam composites

Beatriz Merillas [a,b,c,*], Miguel Ángel Rodríguez-Pérez [a,c], Luisa Durães [b]

[a] Cellular Materials Laboratory (CellMat), Condensed Matter Physics Department, Faculty of Science, University of Valladolid, Campus Miguel Delibes, Paseo de Belén 7, 47011 Valladolid, Spain
[b] University of Coimbra, CERES, Department of Chemical Engineering, Rua Sílvio Lima, 3030-790 Coimbra, Portugal
[c] BioEcoUVA Research Institute on Bioeconomy, University of Valladolid, Spain

ARTICLE INFO

Keywords:
Silica aerogels
Polyurethane foam
Composites
Copper
Adsorption
Isotherms

ABSTRACT

Safe water supply has become one of the main concerns of our society due to the intense industrial activities generating hazardous waste. Among the water pollutants, copper ions are known for potential diseases caused by accumulation of this metal. Therefore, different adsorbents have been produced for this purpose, highlighting aerogels for their effective adsorption owing to their high surface areas and porosity. Herein the synthesis of a novel silica aerogel-based composite for copper removal is described. It was produced by the sol–gel technique, synthesizing the silica aerogel into a reticulated-polyurethane foam that acted as a macrocellular skeleton, preventing a strong shrinkage of the aerogel during the ambient pressure drying. The produced aerogels and composites were characterized in terms of density, textural properties, hydrophobicity, and copper removal efficiency. Isotherm studies revealed a significantly improved adsorption capacity in comparison with the monolithic aerogel, reaching a maximum value of 46.13 mg g^{-1}. The predominant adsorption mechanism was Langmuir- Freundlich adsorption. The adsorption kinetics were also evaluated by different models, as well as the ability to function as filtration medium. Therefore, this work provides a promising strategy for copper uptake avoiding tedious filtration steps to separate the adsorbent, thus reducing time and costs.

Introduction

The increasing industrial and anthropogenic activity levels promote a continuous generation of toxic wastes and sewage leading to worrying water pollution. In fact, according to the World Health Organization (WHO), almost 2 billion people worldwide are consuming contaminated water, causing more than 485,000 human deaths per year and a million marine animals are killed as a consequence of this issue [1]. The consumption of water containing disease-causing microorganisms and poisonous substances can cause immediate and long-term harm to human health, as well as a catastrophic impact on natural ecosystems. There exist different pollutants that are directly released to water such as dyes from the textile industry [2,3], aromatic compounds from the petrochemical activity [4], pesticides from agriculture [5], or heavy metals usually released by metallurgy and mining [6]. These compounds present a real threat to living beings, since they may cause carcinogenic effects in their organisms as well as undesirable diseases. For these reasons, raising awareness of the relevance of developing efficient water-treatments is crucial for providing access to safe water thus promoting health and reducing poverty.

In the recent years, several efforts have been made to enhance the heavy metal removal from soils and water by the development of different adsorbents [7–10]. Nevertheless, aerogels have achieved great attention from the research community since their tailorability, huge specific surface area, and the possibility of chemical functionalization allow them to interact with heavy metals and other pollutants by strong adsorptive interactions [11,12]. Most of these interactions are based on the Irving-Williams rule in which the molecular orbital energy of metal ions is stabilized by donor atoms present in the matrix, such as nitrogen or thiol [13]. According to the adsorbent-adsorbate interactions, the aerogel formulations, especially based on a silica matrix, have been modified by changes in the silane precursors and chemical routes, or the incorporation of functional groups through surface treatments [14]. For instance, epoxy-thiol crosslinking strategies have been employed for

* Corresponding author at: Cellular Materials Laboratory (CellMat), Condensed Matter Physics Department, Faculty of Science, University of Valladolid, Campus Miguel Delibes, Paseo de Belén 7, 47011 Valladolid, Spain.
E-mail address: beatriz.merillas@uva.es (B. Merillas).

https://doi.org/10.1016/j.jiec.2024.11.041
Received 1 October 2024; Received in revised form 7 November 2024; Accepted 19 November 2024
Available online 24 November 2024
1226-086X/© 2024 The Authors. Published by Elsevier B.V. on behalf of The Korean Society of Industrial and Engineering Chemistry. This is an open access article under the CC BY license (http://creativecommons.org/licenses/by/4.0/).

increasing the mechanical stability of the aerogels while presenting efficient dye removals [15].

One of the polluting heavy metals that is causing great attention is copper, owing to its potentially hazardous effects such as the known as "Wilson's disease" [16]. This syndrome, caused by copper accumulation in the organism, especially in the brain, liver, and cornea, promotes neurologic abnormalities (such as Parkinsonism, dysathria, or tremor) affecting the central nervous system, and other problems related to bones, liver, heart and kidney. Copper is explored in hundreds of mines all over the world due to its economic/commercial and technological relevance. The mine tailings, along with metallurgical industry effluents, contribute to the spreading of copper in the soils and water bodies. Therefore, its elimination from water resources poses a high-impact challenge in terms of remediation technologies and health effects in the generalized population. Several researchers have synthesized silica aerogel containing thiol groups by the use of 3-mercaptopropyltrimethoxysilane (MPTMS) as precursor [17,18] or even by in situ epoxy-thiol polymerization as recently reported by Parale et al. [19], or by including amino-based precursors such as 3-aminopropyltrimethoxysilane (APTMS), 3-aminopropyltriethoxysilane (APTES) [20], [3-(trimethoxysilyl)propyl]-ethylenediamine (TMSEN) [21,22], with the aim of removing heavy metals. Nevertheless, despite the enhanced adsorption capacities reached with these materials in comparison with other absorbents such as biochar, activated carbon, or zeolites [23], their applicability is limited to powder forms by milling and grinding the produced aerogels in order to decrease the long-diffusional paths in the material and also to expose more the active sites, thus improving the copper uptake. However, this poses a main drawback of silica aerogels for adsorbing processes, being necessary to perform additional steps such as tedious filtrations for removing the particulate absorbents from the clean water.

Several researchers developed porous polymer monoliths for adsorbing copper ions. For instance, Han et al. [24] synthesized a poly-(glycidyl methacrylate) (PGMA) porous monolith reaching a maximum adsorption capacity of 35.30 mg/g, Wojciechowska et al. [25] reported a maximum adsorption capacity of 1.76 mg/g with gelatin-siloxane hybrid monoliths, and Wang et al. [26] recently presented a gold tailing-based aerogel with an adsorption capacity of 33.51 mg/g. However, these values present room for improvement to comply with the current regulations [27].

For these reasons, the aim of this work is the development of a novel silica-based composite containing nitrogen groups that can be applied in monolithic form during the copper adsorption process with a high performance. Our strategy consists on using reticulated polyurethane foams as scaffold, which allows to maintain the silica aerogel integrity enhancing its mechanical stability. Moreover, the polyurethane skeleton allows to use the ambient pressure drying by protecting the aerogel structure from shrinkage, thus significantly reducing the environmental impact during the synthesis procedure. Despite there exists bibliography in which a polyurethane matrix has been combined with silica aerogels through the incorporation of silica aerogel nanoparticles in the reactive blend [28–30], or by synthesizing hybrid aerogels [31], these strategies imply the modification of the reaction kinetics, morphologies and, therefore, final properties that are not thoroughly under control. For these reasons, in this work, the reticulated polyurethane foams are employed as a supportive skeleton, with no alteration of the aerogel composition and porous structure, constituting a physical reinforcement. The enhanced stability of silica composites introduces the innovative application as monolithic adsorbents, thus avoiding post-filtration processes. Therefore, it contributes to reducing costs and time while keeping a great copper uptake capacity. The obtained results are compared against other silica aerogels reported in the literature for copper adsorption and fitted to different isotherm and kinetic models to determine the adsorption mechanisms. Furthermore, the produced materials have been tested as fast water filters for the first time, reaching promising results for filtering processes as well.

Experimental section

Materials

Polyurethane (PU) reticulated foams were provided by Recticel Iberica, S.L. (Spain). Silica aerogels and silica composites were produced by using 20 % mol TEOS (tetraethyl orthosilicate; $Si(OC_2H_5)_4$; Acros Organics), 60 % mol MTES (methyltriethoxysilane; $CH_3Si(OC_2H_5)_3$; Sigma Aldrich) and 20 % mol APTMS (3-aminopropyltrimethoxysilane; $(CH_3O)_3Si(CH_2)_3NH_2$; Sigma Aldrich), as precursors. The acid catalyst for the sol–gel chemistry was oxalic acid ($C_2H_2O_4$; 99 %; Fluka Analytical) as a 0.01 M aqueous solution. Copper (II) nitrate hemipentahydrate (p.a., Chem-Lab, Zedelgem, Belgium) was used for preparing the heavy metal solutions.

Ethanol (EtOH, absolute, C_2H_5OH) was supplied by Fluka Analytical. High purity water was used whenever needed. Nitric acid (65 %, Fisher) was used to adjust the solutions pH.

Synthesis of aerogel-composites

The synthesis of the silica aerogel-polyurethane foam composites consisted in a two-step sol–gel process [32,33]. First, the corresponding amount of TEOS and MTES were mixed in ethanol. Then, the acidic catalyst (oxalic acid 0.01 M) was added, and the mixture was stirred at 27 °C and 300 rpm for 30 min. Then, the solution was placed in an oven at 27 °C for 24h for hydrolysis. After this time, condensation was promoted under stirring at 300 rpm by the addition of the APTMS precursor acting as a basic catalyst too. The final solution contained 60:20:20 M Si % of MTES, TEOS, APTMS, respectively. The polyurethane foams were placed into the transparent solution that became whitish just before gelation occurred. After reaching the gelation time, gels were placed in an oven at 27 °C for 5 days. Finally, composites were demolded, washed with heptane (2 × 12h) at 50 °C, and dried for 5 h at room temperature, followed by 24 h at 60 °C, and 2 h at 150 °C (see Fig. 1).

Characterization techniques

Bulk density, solid density and aerogel mass

Bulk density (ρ_B) was obtained as the ratio between mass and geometrical volume as described in ASTM D1622/ D1622M-14 [34]. The skeleton density (ρ_S) of the polyurethane foam was taken as 1160 kg/m^3 [35], whereas for the matrix of the silica aerogel, it was measured by helium pycnometry with an AccuPyc II 1340, from Micromeritics, obtaining a value of 1483 ± 34 kg/m^3.

The aerogel mass in the composites was measured as the difference between the initial mass of the polyurethane foams and the final composites according to the following equation:

$$\%\text{aerogel mass} = \frac{(m_{\text{composite}} - m_{\text{foam}})}{m_{\text{composite}}} \quad (1)$$

Scanning electron microscopy

The structure of the silica aerogels, polyurethane foams, and produced composites was observed by using a scanning electron microscope (ESEM Scanning Electron Microscope QUANTA 200 FEG, Hillsboro, OR, USA and FlexSEM 1000, Hitachi). Before the visualization, samples were metallized with iridium [36].

Specific surface area (S_{BET}) and pore size

Nitrogen sorption measurements were performed with a Micromeritics (ASAP 2020) instrument. First, the samples were degassed under vacuum at 25 °C for 24h and then experiments were carried out at – 196 °C in the range of $P/P_0 = 0.05–0.30$ (P_0 is the saturation pressure of N_2 at −196 °C). The specific surface area was obtained by the Brunauer-Emmett-Teller (BET) method [37].

The pore size of the reticulated polyurethane foams was measured by

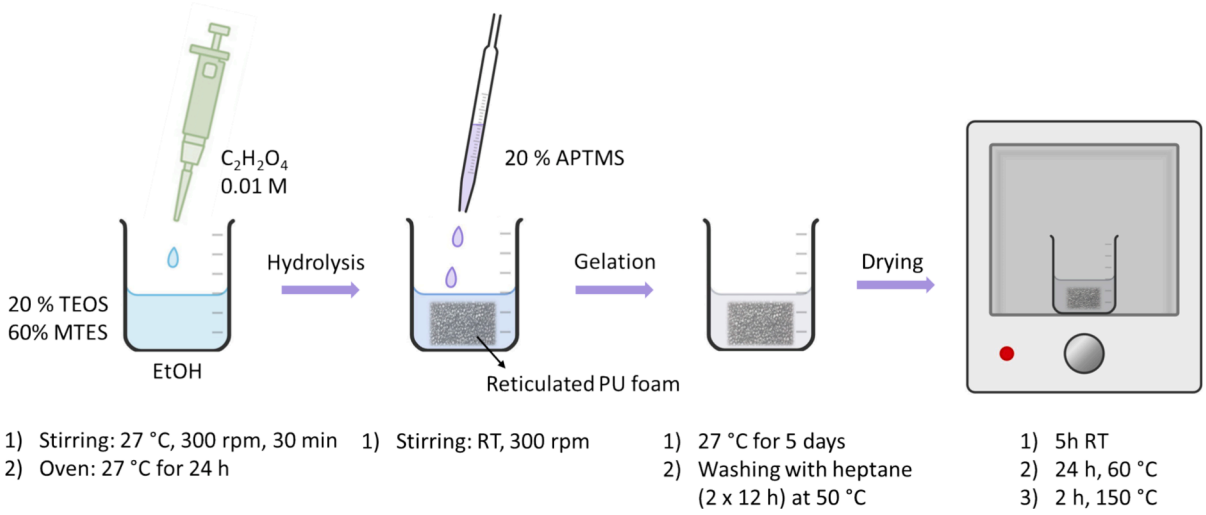

Fig. 1. Synthesis scheme for silica aerogel-polyurethane foam composites.

the SEM pictures by using a software based on IMAGE/J [38]. For the silica aerogels, pore size (Φ_{pore}) was calculated by equation (2):

$$\Phi_{pore} = \frac{4V_p}{S_{BET}} \quad (2)$$

Where S_{BET} is the specific surface area and V_p the total pore volume, the latter being determined as the gaseous volume per unit of mass by subtracting the skeleton volume from the total volume of the monolith (equation (3):

$$V_p = \frac{1}{\rho_B} - \frac{1}{\rho_s} \quad (3)$$

Contact angle

The degree of hydrophobicity was determined through the sessile drop method by suspending a 15 μL pure water droplet on the sample surface [39]. The contact angle measurements were carried out by the IMAGE/J software from a taken photograph.

Atomic absorption spectroscopy

Copper concentration in solution was determined by flame atomic absorption spectroscopy (Perkin-Elmer, PinAAcle 500 model). A Perkin-Elmer Intensitron Hollow Cathode lamp was used with 324.75 nm wavelength. A calibration was performed with five standard solutions (0.5, 1, 2, 4 e 5 mg·L^{-1}) (Spectrosol BDH).

Adsorption experiments

1.83 g of copper(II) nitrate hemipentahydrate was dissolved in Milli-Q ultrapure water for obtaining a stock solution of 1000 mg·L^{-1} (0.5 L). From this initial solution, the other solutions of this work were prepared (10, 20, 50, 100, 150, 200 mg·L^{-1}), and their pH was adjusted by nitric acid to 3.5. All the adsorption experiments were carried out by placing in contact 45 mL of the corresponding solution in glass flasks with 0.09 g of the adsorbent (foam or silica aerogel) to keep a solid/liquid ratio of 2 g adsorbent/L solution. With the aim of comparing between samples, the composite mass used for the adsorption tests was that containing 0.09 g of silica aerogel inside the composite, considering the aerogel mass percentage included in the final composite. These solutions were continuously stirred in a rotational stirrer at 30 rpm (REAX 20, Heidolph Instruments, Schwabach, Germany).

Adsorption isotherms. Copper adsorption isotherm experiments were performed at room temperature using the batch equilibrium technique. 45 mL of solution (concentrations of 10, 20, 50, 100, 150, 200 mg·L^{-1}) was placed in contact with 0.09 g of the corresponding adsorbent (polyurethane foam, silica aerogel, or aerogel in the composite form) in 50 mL flasks. The solid–liquid systems were stirred for 24 h in order to guarantee that the sorption equilibrium was reached. Each concentration and adsorbent type was evaluated in duplicate to ensure greater reliability.

The adsorption capacity (q_e) was determined by equation (4) and expressed as mg of removed adsorbate per grams of adsorbent:

$$q_e = \frac{(C_0 - C_e)*V}{m_{adsorbent}} \quad (4)$$

Where C_0 and C_e are the initial and equilibrium concentrations, respectively, V is the total volume (L), and $m_{adsorbent}$ the grams of adsorbent.

The removal percentage was calculated according to equation (5):

$$Removal(\%) = \frac{(C_0 - C_e)}{C_0} \cdot 100 \quad (5)$$

Adsorption kinetics. For the adsorption kinetic experiments, a solution of 50 mg·L^{-1} was placed in contact with the composite adsorbent at 30 rpm and different incubation times: 5, 10, 20, 60, 120, 180, 300, 800, and 1440 min. The solid/liquid ratio was maintained as 2 g/L. The sorbate uptake at a given time (t expressed in minutes) was given by q_t (mg/g) that was calculated analogously than q_e being C_t the concentration at a time t.

Fourier transform infrared spectroscopy (FTIR)

FTIR spectra of the silica aerogel-polyurethane foam composites were collected using a Bruker Tensor 27 spectrometer working in Attenuated Total Reflectance (ATR) method with an MKII Golden-Gate accessory. Each spectrum was obtained at room temperature after 32 scans and a resolution of 4 cm^{-1} in the range 600–4000 cm^{-1}.

Results and discussion

Materials characterization

The polyurethane foams, monolithic silica aerogels, and silica aerogel-polyurethane foam composites have been characterized in detail. The main properties of these materials are gathered in Table 1. It can be observed a significant increase in the density of the silica aerogel-polyurethane foam (Sil-PU) composite with respect to the initial foam, going from 29.4 ± 0.3 kg/m^3 to 70.2 ± 1.3 kg/m^3 as a consequence of the aerogel mass contained in the composite. The aerogel mass percentage included in the composites was calculated by equation (1),

Table 1
Main properties of the produced aerogels.

Sample	ρ_B (kg/m^3)	Porosity (%)	Aerogel mass (%)	S_{BET} (m^2/g)	V_p (cm^3/g)	Mean pore size (nm)	Water Contact angle (°)
PU foam	29.4 ± 0.3	97.5	0	3.91 ± 0.20	33.62	435 × 10^3	129.8
Silica aerogel	375.7 ± 27.8	74.7	100	10.29 ± 0.03	1.99	772	124.7
Si-PU composite	70.2 ± 1.3	94.9	69.7 ± 0.4	99.32 ± 0.30	13.51	546	129.2

obtaining an average value of ca. 70 % in all the samples, which accounts for the high amount of foam pores that have been filled with the aerogel.

The hydrophobicity of the produced materials was determined by the contact angle method. For all the materials, aerogel, foam and composites, the water contact angles are in the interval 120-130° (Fig. 2**a,** Table 1), being considered as hydrophobic materials according to the IUPAC classification. This nature of the compounds allows them to maintain their integrity during the adsorption process, their structures not being affected by the medium. For composites with a lower hydrophobicity degree, the interactions between the aerogel and water would lead to poor mechanical stability and the release of small aerogel particles in the adsorption medium.

Textural properties and porous structures

Regarding the textural properties, the specific surface area of the foam, aerogel and composite was measured by nitrogen sorption. The polyurethane foam and the pure silica aerogel showed a significantly small specific surface area of 3.91 and 10.3 m^2/g, respectively. The low specific surface area of the pure aerogel is a consequence of the huge shrinkage experimented during the ambient pressure drying process. It should be also noted that the incorporation of amine groups in silica-based aerogels always brings a detrimental effect on the specific surface area [40]. Nevertheless, the Sil-PU composites showed a remarkably higher surface area with 99.3 m^2/g. This higher value is explained by two different effects; the non-filled pores of the polyurethane foam that are increasing this parameter, and the reduced shrinkage of the aerogel when being scaffolded by the polyurethane skeleton, thus reducing its average density, and increasing the surface area.

The obtained pore volumes also indicate this shrinkage reduction for the composite, increasing the pore volume from 1.99 to 13.5 cm^3/g. This higher pore volume, combined with smaller pores, leads to the observed increase in the specific surface area. Indeed, the porosity of the composite was 94.9 %, obtaining a remarkable increment with respect to the silica aerogel porosity of 74.7 %. Thus, the possibility of drying these composites by ambient pressure method reduces the environmental impact and energy consumption while keeping good textural properties.

The porous structures of the produced materials were evaluated by the scanning electron micrographs (**Figure S1 of Supporting Information**). Fig. 2**b** displays the structure of the silica aerogel-polyurethane foam composite. It can be clearly seen the silica aerogel pieces (grey colour) inside the foam cells and attached to the cell struts (orange colour). The non-filled pores favor water penetration, increasing the contact surface of the aerogel with the polluted water solution. Furthermore, a magnification of the aerogel structure is also shown in

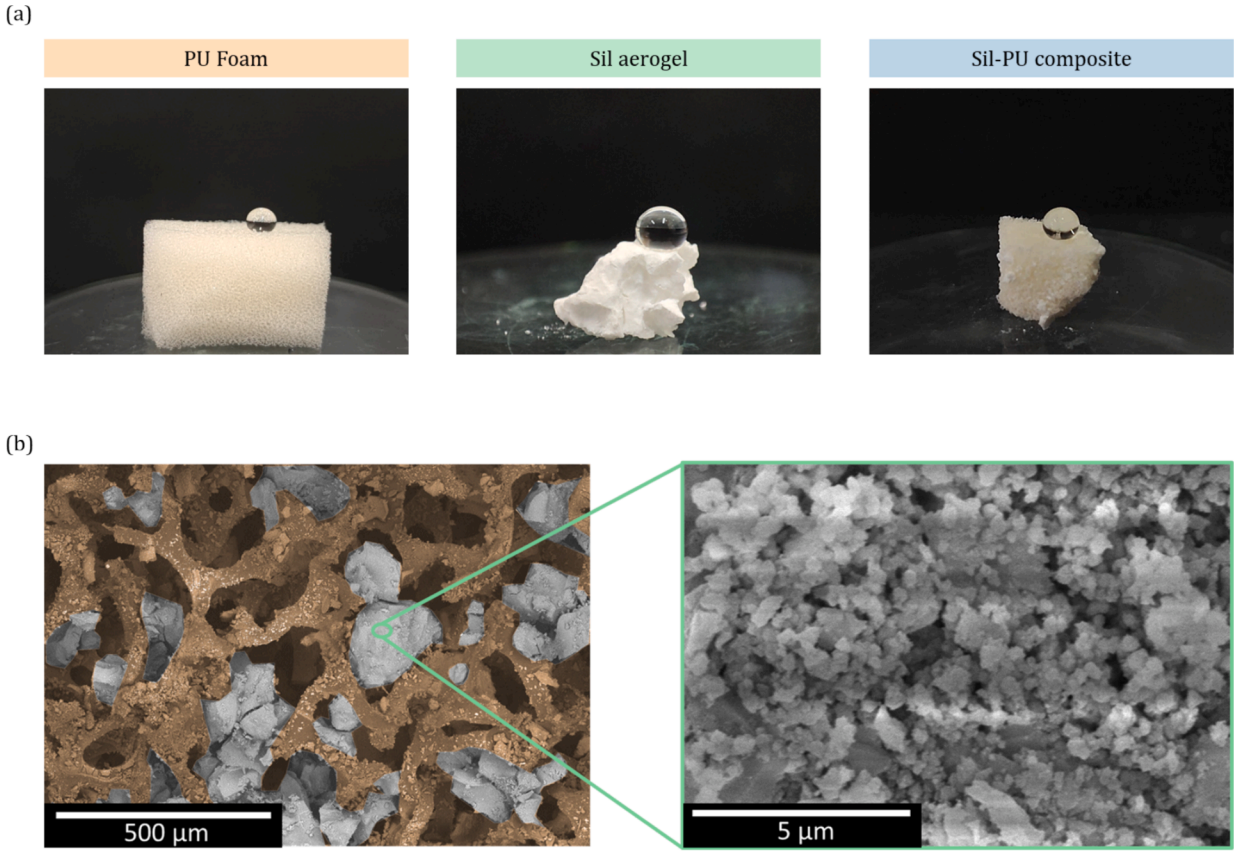

Fig. 2. a) water droplet on the surface of the polyurethane foam (left), silica aerogel (middle), and composite (right); b) scanning electron micrograph of the polyurethane foam-silica aerogel composite with a magnification of the silica aerogel.

Fig. 2**b**, showing the pearl-necklace structure of the silica network formed by particles (average particle size of 250 nm). Silica secondary particles of such large size are typical of the amine groups catalytic effect on condensation reactions [41].

Adsorption equilibrium experiments: Isotherms

The adsorption experiments were carried out by using the same mass of active species, as indicated in section 2.3.6. The employed materials before and after adsorption are shown in Fig. 3**a**. Moreover, the infrared spectra of the composites before and after the adsorption process are provided at **Figure S2** showing the characteristic peaks corresponding to the chemical structure that does not change during the procedure. According to the appearance of the materials after the adsorption equilibrium experiments, it is suggested that the polyurethane foams do not have interactions with the copper cations. Nevertheless, the Sil-PU composite and silica aerogel present a blue colour owing to the adsorption of this metal. Then, the adsorption isotherms by using different copper concentrations for 24h were obtained for the three materials under study. The pH value of 3.5 was chosen to avoid the competition of H^+ for the active sites occurring usually at pH below 2 [42], and the formation of metal hydroxides that can occur above pH 4 as demonstrated by a Štandeker et al. [17]. The appearance of the final aerogels and composites can be observed in Fig. 3**b** and Fig. 3**c**, respectively.

Regarding the copper adsorption removal plotted in Fig. 4**a**, it can be seen that the polyurethane foam presents a removal percentage of almost 0 % for all the selected concentrations. Therefore, despite the presence of nitrogen groups of the urethane chain of these polyurethane foams, copper is not able to interact with these chemical groups. The monolithic silica aerogel showed remarkably low removal percentages of ca. 3 % for 10 and 20 $mg{\cdot}L^{-1}$ solutions, whereas this removal decreases to ca. 1 % when increasing the copper concentration over these values. This fact is likely due to the low specific surface area of these monoliths, and the small pore volume that they contain owing to the strong shrinkage occurring during drying. In the case of the Sil-PU composites, the removal percentage is notably higher; the maximum removal was 88 %, reached for the minimum initial concentration of 10 $mg{\cdot}L^{-1}$, which slightly decreases to ca. 78 % for the successive concentrations of 20, 50, and 100 $mg{\cdot}L^{-1}$. Then, this value experiments a sharper drop down to 55 % for 150 $mg{\cdot}L^{-1}$ and 46 % for the maximum concentration of 200 $mg{\cdot}L^{-1}$, most likely due to the depletion of active sites. Then, the adsorption capacities were evaluated by equation (4), obtaining the data represented in Fig. 4**b**. As expected, the adsorption capacities of PU foams were residual. In the case of monolithic aerogel, these did not exceed the value of 1 $mg{\cdot}g^{-1}$. However, the produced composites demonstrated an excellent adsorption capacity for copper that rises from 4.4 $mg{\cdot}g^{-1}$ for the minimum concentration, to 46.1 $mg{\cdot}g^{-1}$ for 200 $mg{\cdot}L^{-1}$. The possibility of adsorbing copper on these materials (aerogel and composites) is given by the presence of primary amine groups of the APTMS precursor, that interact with copper cations in solution. The main difference in the adsorption capacity between these materials is due to the exposed surface area. As explained in section 3.1.1, the monolithic silica aerogels present a reduced specific surface area because of the strong shrinkage during the drying procedure, which promotes the densification of the structure, thus, hindering

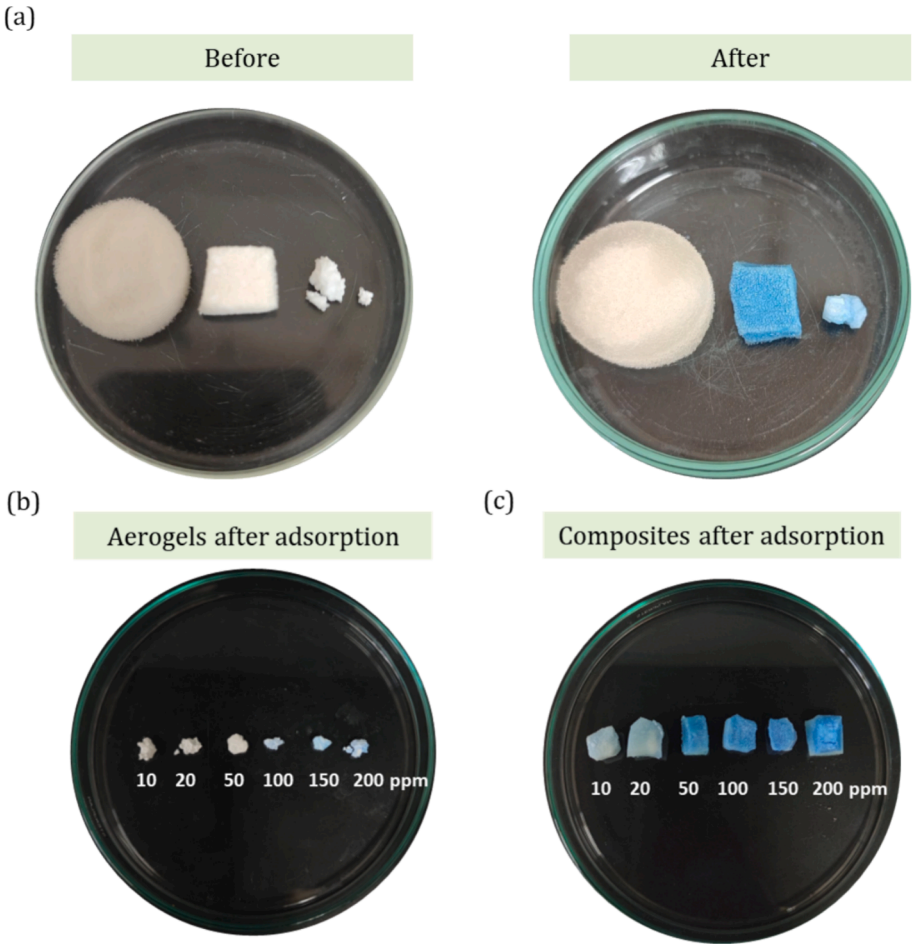

Fig. 3. (a) Selected mass of each material for the copper adsorption experiments before and after adsorption; (b) Aerogel materials after copper adsorption at different initial concentrations; (c) Composites materials after copper adsorption at different initial concentrations.

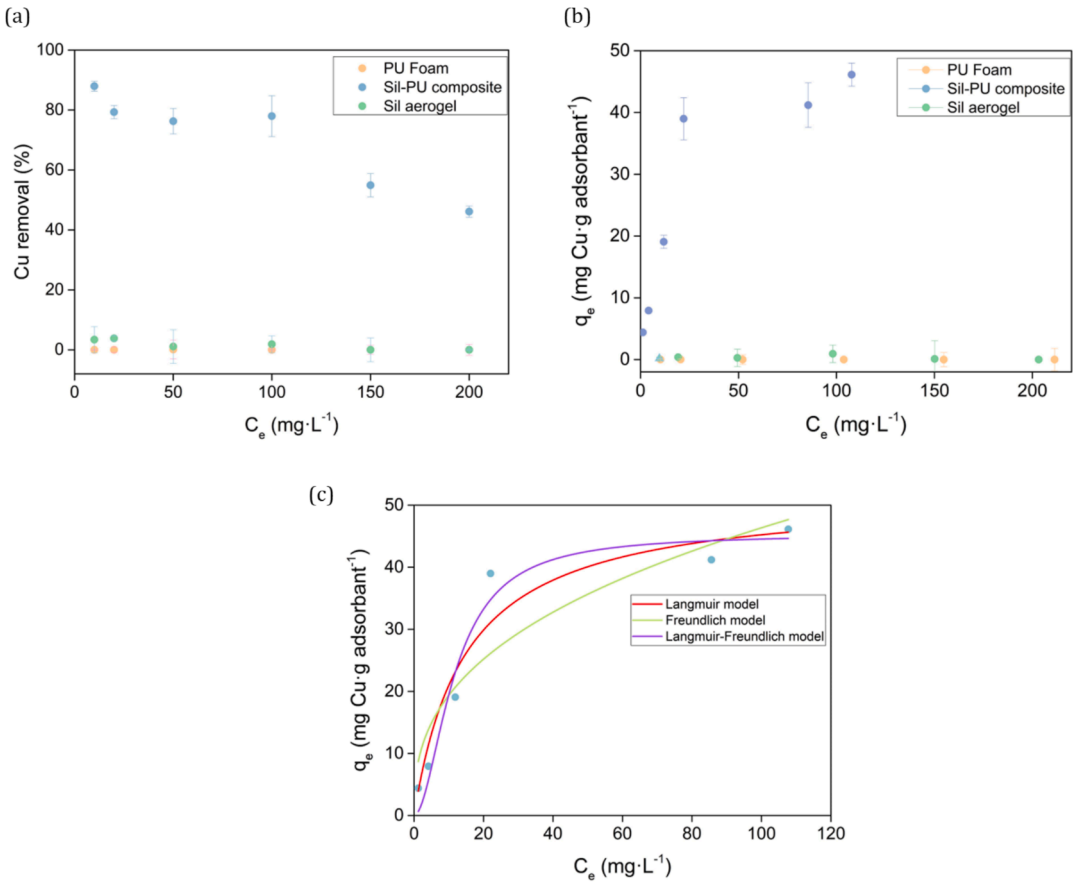

Fig. 4. Copper equilibrium adsorption isotherms: a) Removal % of all the compounds; b) adsorption capacity of all the compounds; c) Adsorption isotherms and fitting models for the Sil-PU composites.

the access to the functional groups (Fig. 5**a**) for the metal adsorption. Moreover, the diffusional path to the inner active sites is long, and there is obstruction of the pore entry regions by copper ions. Nevertheless, the produced composites present a 10-fold increase in the specific surface area, leading to the exposure of more active sites and shortening of diffusional paths, thus favouring the adsorption process (Fig. 5**b**).

The most common empirical adsorption models (Langmuir [43], Freundlich [44], and Sips [45] models) were fitted to the data using the corresponding equations [46]. The Langmuir model follows a type-I isotherm (according to the IUPAC classification [47]) that reaches a horizontal asymptote when the adsorbate forms a monolayer (equation (6).

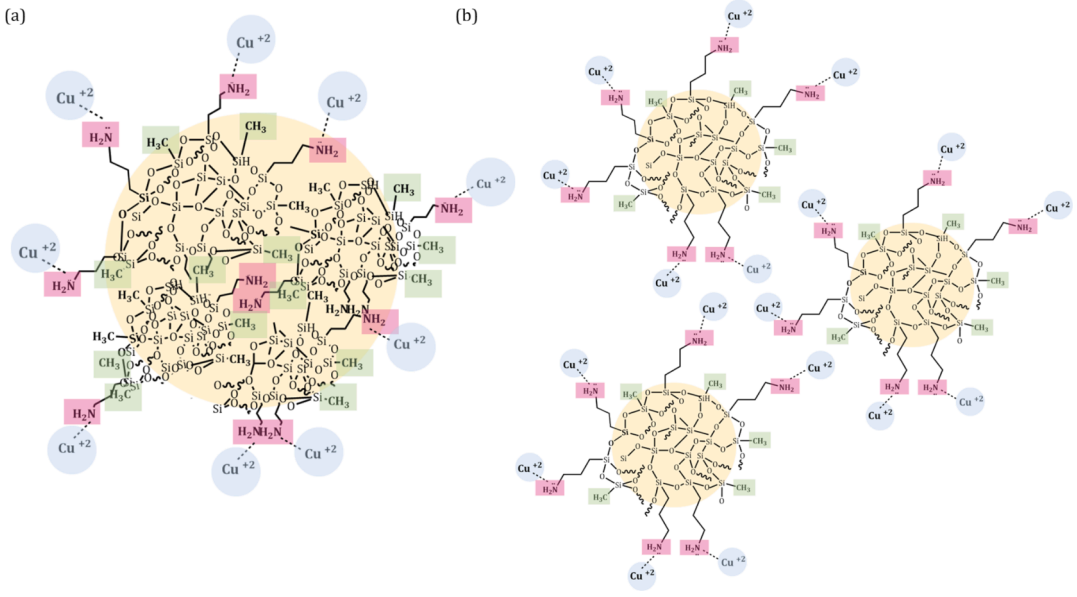

Fig. 5. Simulation of chemical groups interaction with copper ions in the (a) silica aerogel monolith, and the (b) Sil-PU composite.

$$q_e = \frac{q_m \cdot K_L \cdot C_e}{1 + (K_L \cdot C_e)} \quad (6)$$

Where K_L (L·mg^{-1}) is the Langmuir constant, q_m (mg·g^{-1}) is the maximum adsorption capacity, and C_e is the equilibrium concentration (mg·L^{-1}).

The Freundlich isotherm model accounts for surface heterogeneity as a result of a multilayer adsorption type and is described by equation (7):

$$q_e = K_F \cdot C_e^{\frac{1}{n_F}} \quad (7)$$

Where K_F is the Freundlich constant ((mg·g^{-1})·(L·mg^{-1})$^{1/n_F}$), and n_F the heterogeneity factor.

The Sips model is widely used for interpreting the adsorption data by a combination of the previously described models, Langmuir and Freundlich for a single component. The isotherm can be expressed as:

$$q_e = \frac{q_m \cdot K_S \cdot C^{\frac{1}{n}}}{1 + K_S \cdot C^{\frac{1}{n}}} \quad (8)$$

Where q_m (mg·g^{-1}) is the maximum adsorption capacity associated with the total number of binding sites, K_S the Sips isotherm constant, and n the Sips heterogeneity factor.

The fitting accuracy of each model was assessed by the Akaike and Bayesian criteria (AIC, BIC) and *R*-squared [48].

The adsorption isotherm curves for the Sil-PU composites are displayed in Fig. 4**c** and the fitting parameters are gathered in Table 2. Despite the AIC and BIC criteria suggesting Langmuir as the main model, results indicate that the Langmuir-Freundlich combination model is the best fitting model for the data obtained from the experiments, indicating a heterogeneous adsorption mechanism at low concentrations, and monolayer adsorption at higher concentrations on the amine-group active sites in a similar manner as the Langmuir isotherm. Once these sites are saturated, a maximum adsorption capacity of 45.33 (mg·g^{-1}) would be reached.

A comparison with the adsorption capacity values found in the literature for aerogel-based materials in copper removal from water was performed and the values are reported in Table 3. There is a wide range of adsorption capacities comprised between 140 and 1.50 (mg·g^{-1}). Nevertheless, it should be noted that all the materials presented as adsorbents (except the work of Pouretedal and Kazemi [18] and Jiao et al. [49] in which it is not specified) are employed in powder form after milling and grinding processes leading to small particles or beads that require additional and tedious filtration steps to recover a clean solution free of adsorbent materials. The main advantage of the composite presented in this work lies in the avoidance of filtration steps, being easily recovered after the adsorption processes. In comparison with the adsorption capacities, these Sil-PU composites present similar values to those obtained in other works [17,50,51]. Most of the materials presenting higher capacities are produced by supercritical drying which leads to higher specific surface areas. However, the use of that drying technique significantly increases the production complexity and costs. Thus, the production of the presented aerogel-containing composites constitutes an interesting alternative to other aerogel-based adsorbents presented in the literature, characterized by a cost-effective production process following ambient pressure drying and the saving of tedious milling and filtering steps.

Table 3
Equilibrium adsorption capacities of aerogel-based materials for copper adsorption experiments from the literature.

Type of adsorbent material	Drying method[(a)]	pH	q_e (mg·g^{-1}).	Ref.
Milled silica aerogel (powder 75–250 μm) with amino groups	APD	5.5	140	[22]
Silica aerogels containing mercapto groups	APD	6	90.1	[18]
Milled silica aerogel (powder below 250 μm) with amino groups	APD	6	47.6	[51]
Silica aerogel-reticulated PU foam composite	APD	3.5	46.13	This work
Polybenzoxazine aerogel (particle size less than 150 μm)	APD	4–5	1.50	[52]
Milled silica aerogel (powder 75–250 μm) with amino groups	SCD	5	124.2	[53]
Milled silica aerogel (powder 75–250 μm) with amino groups	SCD	5	117.0	[40]
Milled silica aerogel (powder 75–250 μm) with amino groups	SCD and APD	4–5	56.0	[50]
Silica aerogels containing mercapto groups in powder (smaller than 0.25 mm)	SCD	4–6	51.02	[17]
Alginate aerogel beads	SCD	4.5	126.8	[54]
Sodium alginate/graphene oxide aerogel	FD	5	98.0	[49]

(a) SCD: supercritical drying, APD: ambient pressure drying, FD: freeze drying.

Adsorption kinetics

According to the obtained results for the different copper concentrations, the concentration of 50 mg·L^{-1} was selected to perform the kinetic experiments, following the copper adsorption by the Sil-PU composite materials as a function of time. Each time was repeated twice in order to obtain an average value with higher reliability. As can be seen in Fig. 6**a**, copper removal followed an initially fast uptake, removing 20 % of the total copper amount after 120 min and 70 % after 300 min, a behaviour already observed by other authors [52,55] for copper uptaking. From this time on, adsorption kinetics gradually slows down reaching a steady state or ca. 72 % at 800 min and 76 % at 1440 min. These experiments prove the excellent copper uptake reached by the silica aerogel-polyurethane foam composites as a result of the enhanced water contact with the material surface and the stability of these materials due to their hydrophobic nature.

Different adsorption kinetic models were fitted to data, according to equations (9) to (12). The Lagergren model, known as the pseudo-first order [56] that generally describes the adsorption process by physisorption onto the adsorbent surface (equation (9), and the Ho-McKay model or pseudo-second order model [57], describing the rate-limiting mechanism of adsorption by chemisorption (equation (10), were used.

$$q_t = q_e(1 - e^{-t \cdot k_1}) \quad (9)$$

Where q_e (mg·g^{-1}) is the adsorption capacity at equilibrium and q_t

Table 2
Fitting parameters for the adsorption isotherm models.

Parameters	Langmuir model	Parameters	Freundlich model	Parameters	Sips model
q_{max} (mg·g^{-1})	51.88	$1/n_F$	0.38	q_{max} (mg·g^{-1})	45.33
K_L (L·mg^{-1}) × 10^3	67.89	K_F (mg·g^{-1})·(L·mg^{-1})$^{1/nF}$	8.10	K_S (mg·g^{-1}) × 10^3	10.17
				$1/n$	1.87
AIC	34.93	AIC	39.88	AIC	62.24
BIC	22.30	BIC	27.26	BIC	21.41
R^2	0.92	R^2	0.83	R^2	0.93

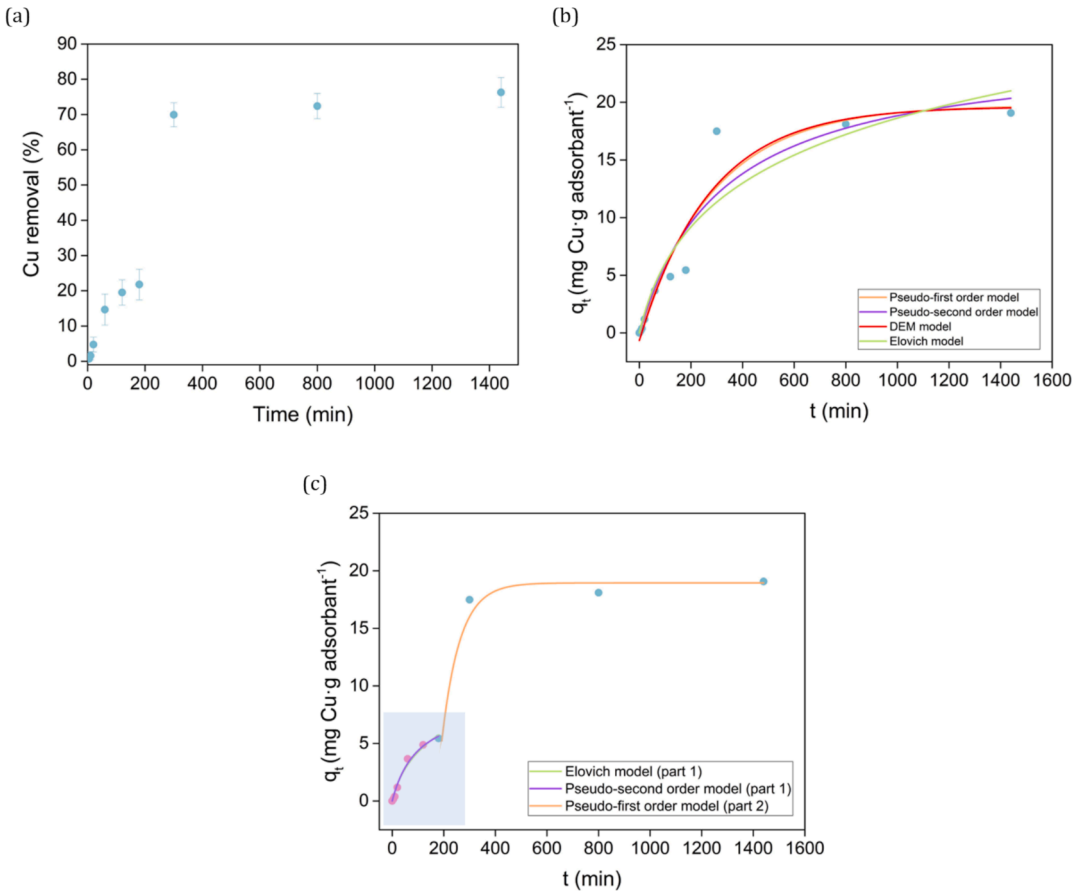

Fig. 6. (a) Copper removal kinetics; (b) Adsorption kinetics with global fitting; (c) Adsorption kinetics with split fitting, of Sil-PU composites. The concentration of the Cu^{2+} was 50 mg·L^{-1}.

(mg·g^{-1}) at a given time (t), and k_1 is the first order constant (min^{-1}).

$$q_t = \frac{q_e^2 \cdot k_2 \cdot t}{1 + q_e \cdot k_2 \cdot t} \tag{10}$$

Where k_2 is the pseudo-second order rate constant (g·mg^{-1}· min^{-1}).

Then, the double exponential model (DEM, equation (11) is employed to describe adsorption processes based on a two-step mechanism with a fast beginning and a slower secondary step towards equilibrium [58].

$$q_t = q_e - \frac{D_1}{c} \cdot e^{-K_{D1} \cdot t} - \frac{D_2}{c} \cdot e^{-K_{D2} \cdot t} \tag{11}$$

Where K_D is the adsorption constant rate that is related to the diffusivity mechanism (min^{-1}), c is the adsorbent concentration (mg·L^{-1}), and D_1 and D_2 represent the maximum adsorbed amount (mg·L^{-1}).

Finally, the Elovich model that assumes an adsorption rate exponentially decreasing with the amount of adsorbed solute was fitted (equation (12) [59].

$$q_t = \frac{1}{b} \cdot \ln(1 + a \cdot b \cdot t) \tag{12}$$

The four non-linear regression models previously described were fitted to the data, however, by observing Fig. 6**b**, it is noticed that none of these models satisfactorily described the kinetic mechanism (all the parameters can be found in **Table S1 of Supporting Information**). The obtained results reveal two different tendencies. Therefore, a mixed model was taken to describe the kinetics of the copper adsorption by these materials. Fig. 6**c** shows the best models fitting the two-step behaviour.

The first points of the adsorption process, from 0 to 180 min, were fitted by the Elovich model and the pseudo-second order model reaching a good correlation for both models. A comparison between models was performed in order to determine the one that better describes the adsorption mechanism at early stages (Table 4). According to the Akaike and Bayesian Information Criteria, the pseudo-second order rate is driving the copper adsorption by chemisorption on the binding sites. This model is typical for heavy metal adsorption as demonstrated by Vareda et al. [7]. These interactions are undertaken by the primary amine groups of the APTMS that act as Lewis bases while copper cations act as Lewis acids and their interactions are described by Pearson's Hard and Soft Acids and Bases theory [60]. Consequently, it could be hypothesized that this mechanism might be responsible for the formation of the early-stage monolayer on the composite surface.

Then, the binding of the subsequent copper cations in stage 2 (180 – 1440 min) is described by the pseudo-first order model. This behaviour has been recently observed by other authors such as Ezzati et al. [61] and Valente et al. [62] in adsorption tests, explaining that this model can describe the adsorption process when the system is approaching to equilibrium. Thus, the chemisorption mechanism changes to physisorption once the binding sites are occupied close to the equilibrium stage. Therefore, a mixed model pseudo-second order/pseudo-first order is the one describing the adsorption kinetics of the Sil-PU composites produced in this work.

Sil-PU composites as fast filters for copper removal from water: A proof of concept

The produced Sil-PU composites were easily cut with scissors to the size of a plastic syringe (Fig. 7**a**). Samples showed proper adaptability in

Table 4
Fit parameters for sorption kinetic models of Fig. 6**c**.

1st stage				2nd stage	
Parameters	**Pseudo-second order model**	**Parameters**	**Elovich model**	**Parameters**	**Pseudo-first order model**
q_e (mg·g^{-1})	8.84	a (mg·g^{-1}·min^{-1})	0.092	q_e (mg·g^{-1})	14.197
k_2 (g·mg^{-1}·min^{-1}) × 10^3	1.11	b (g·mg^{-1})	0.322	k_1 × 10^3 (min^{-1})	14.340
AIC	−4.69	AIC	−2.57		
BIC	−12.85	BIC	−10.73		
R^2	0.982	R^2	0.976	R^2	0.864

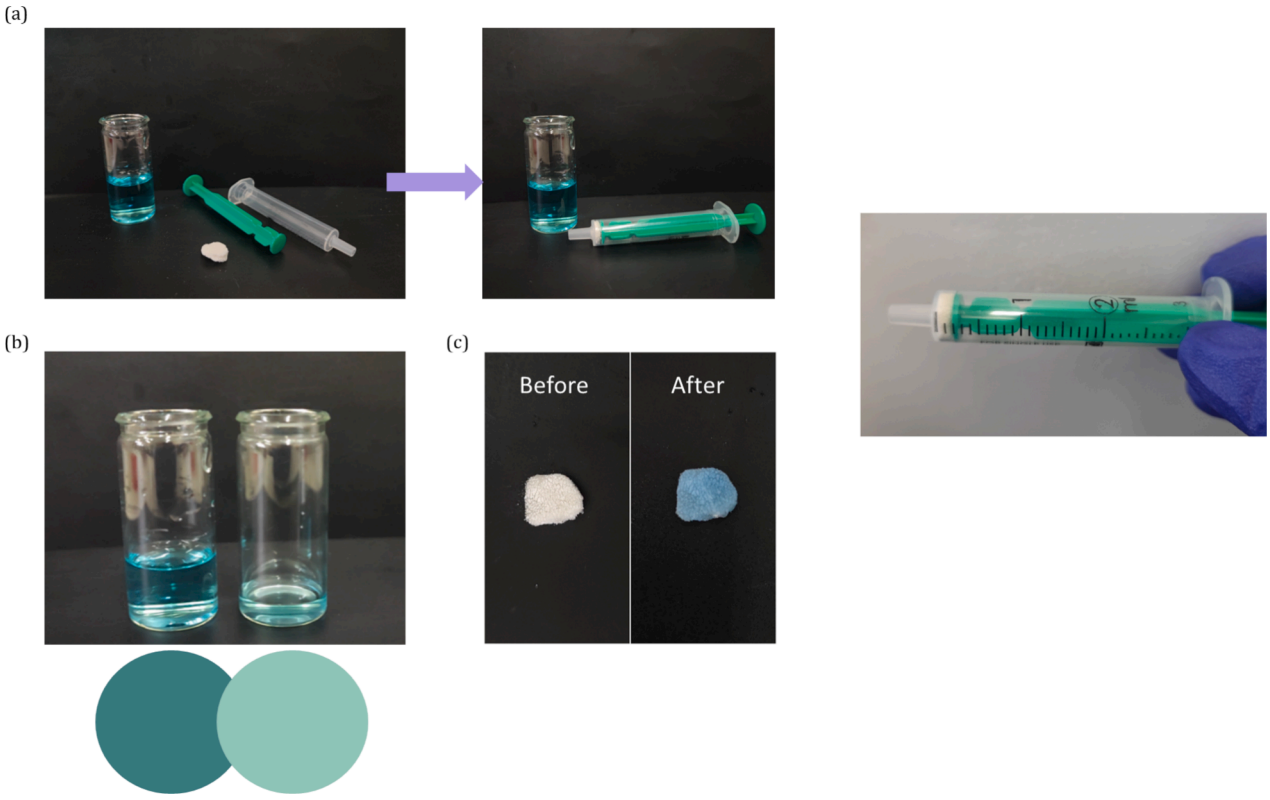

Fig. 7. (a) Filter setting into a syringe; (b) Qualitative colourimetric example of filtration; (c) Sil-PU composite before and after a fast filtration.

shape to act as filters when passing a polluted solution with a high concentration of copper ions. As a proof of concept, these filters were used to clean a highly concentrated solution dropping into another vial the filtered solution. It was proved by colourimetric analysis that the copper concentration was significantly reduced (Fig. 7**b**) obtaining a blue-coloured filter after the filtration process as a result of the adsorption as shown in Fig. 7**c**. Moreover, the channels between the aerogel and the foam allow to decrease the head loss through the material to feasible values.

Thus, since these composites are promising materials for fast filters, a thorough study is being conducted by the authors by checking all the affecting parameters of the filtration process, such as contact time, filter thickness, solution volume, reproducibility, and reusability.

Conclusions

A novel silica aerogel-polyurethane foam composite has been synthesized for an efficient copper adsorption from water. The composite included a silane precursor containing amino groups to promote the metal-nitrogen interactions, and tetraethyl orthosilicate combined with methyltriethoxysilane to induce a balance of hydrophilicity/hydrophobicity. This aerogel was produced into a reticulated polyurethane foam that acted as a skeleton protecting the integrity of the silica aerogel and reducing the experimented shrinkage during the ambient pressure drying process, which increased its specific surface area from 10.3 to 99.3 $m^2 \cdot g^{-1}$, and total pore volume from 1.99 to 13.5 $cm^3 \cdot g^{-1}$.

The produced materials showed a significantly improved adsorption capacity in comparison with the monolithic aerogel, going from values below 1 mg·g^{-1} for the pure aerogel to 46.1 mg·g^{-1} for the composite at 200 mg·L^{-1}. High percentage removals were obtained, reaching 90 % for concentrations of 10 mg·L^{-1}, and decreasing to 46 % for the maximum concentration (200 mg·L^{-1}). After applying different models, the adsorption mechanism was described by the Sips model. Therefore, a combination of Langmuir-Freundlich mechanisms dominates the process, where a monolayer of adsorbate will be formed in the active sites of the composite at high concentrations until being saturated. The adsorption kinetics were described by a combination of models: the first step of fast uptaking (0–180 min) fitted to the pseudo-second order model, suggesting a chemisorption mechanism; the second stage (180–1440 min), presenting a slower rate, was described by the pseudo-first order model, a typical behaviour when equilibrium is being reached.

Therefore, the polluted water-aerogel interaction was favoured by the employment of the Sil-PU composite, presenting a high copper uptake in monolithic form. Thus, this strategy avoids tedious previous grinding steps and final filtration after the adsorption process which

would increase time and costs.

Additionally, the produced materials were tested as fast filters for polluted water showing a promising behavior by colorimetric analysis. Thus, not only do these composites reduce additional steps during adsorption processes, but they can also be used in monolithic form for fast and effective filtrations, showing great adaptability to the filtering setup. These studies will be further conducted by the authors to perform a detailed analysis of the different parameters affecting filtration with these composites.

Funding

Work carried out in the frame of the COST Action "Advanced Engineering and Research of aeroGels for Environment and Life Sciences" (AERoGELS) and funded by the European Commission under grant agreement No. CA18125. Financial assistance from Ministerio de Ciencia, Innovación y Universidades (MCIU) (Spain) (PID2021-127108OB-I00, TED2021-130965B-I00, PID2020-120010RB-I0 and PDC2022-133391-I00), Regional Government of Castilla y León and the EU-FEDER program (CLU-2019–04 and VA202P20) are gratefully acknowledged. This work was supported by the Regional Government of Castilla y León (Junta de Castilla y León), and by the Ministry of Science and Innovation MICIN and the European Union NextGenerationEU / PRTR. (C17. I1). CERES research unit was supported by national funds from FCT – Fundação para a Ciência e a Tecnologia, I.P., and when appropriate co-funded by the European Regional Development Fund (ERDF), under the scope of projects https://doi.org/10.54499/UIDB/00102/2020 and https://doi.org/10.54499/UIDP/00102/2020.

CRediT authorship contribution statement

Beatriz Merillas: Writing – review & editing, Writing – original draft, Visualization, Validation, Methodology, Investigation, Formal analysis, Data curation, Conceptualization. **Miguel Ángel Rodríguez-Pérez:** Writing – review & editing, Supervision, Resources, Project administration, Funding acquisition, Conceptualization. **Luisa Durães:** Writing – review & editing, Supervision, Resources, Project administration, Methodology, Funding acquisition, Conceptualization.

Declaration of competing interest

The authors declare that they have no known competing financial interests or personal relationships that could have appeared to influence the work reported in this paper.

Acknowledgements

The authors would like to thank María Dolores Marqués Gutiérrez, from the Porous Solids Laboratory of the University of Malaga, for the nitrogen adsorption measurements, and Fernando González, from the Unidad de Microscopía of the Parque Científico of the University of Valladolid, for the HR-SEM images and Pablo Obregón Sandoval for the SEM (FlexSEM 1000, Hitachi) measurements.

Appendix A. Supplementary data

Supplementary data to this article can be found online at https://doi.org/10.1016/j.jiec.2024.11.041.

References

[1] World Health Organization, Drinking-Water , Sanitation and Health, 2011.
[2] F. Amalina, A.S.A. Razak, S. Krishnan, A.W. Zularisam, M. Nasrullah, Dyes removal from textile wastewater by agricultural waste as an absorbent – A review, Clean. Waste Syst. 3 (2022) 100051, https://doi.org/10.1016/j.clwas.2022.100051.
[3] M.T. Yagub, T.K. Sen, S. Afroze, H.M. Ang, Dye and its removal from aqueous solution by adsorption: A review, Adv. Colloid Interface Sci. 209 (2014) 172–184, https://doi.org/10.1016/j.cis.2014.04.002.
[4] C.M.C. Filho, T. Matias, L. Durães, A.J.M. Valente, Efficient simultaneous removal of petroleum hydrocarbon pollutants by a hydrophobic silica aerogel-like material, Colloids Surf. A Physicochem. Eng. Asp. 520 (2017) 550–560, https://doi.org/10.1016/j.colsurfa.2017.02.018.
[5] N.I.W. Azelee, N.H.A. Manas, S.Z. Hanapi, S.H.M. Sarip, R.A. Malek, H.A. El-Enshasy, D.J. Dailin, M.F. Ngah, Removal of pesticides from water and wastewater by agricultural biomass-based adsorbents, INC (2022), https://doi.org/10.1016/B978-0-323-90893-1.00017-9.
[6] M.O. Fashola, V.M. Ngole-Jeme, O.O. Babalola, Heavy metal pollution from gold mines: Environmental effects and bacterial strategies for resistance, Int. J. Environ. Res. Public Health. 13 (2016), https://doi.org/10.3390/ijerph13111047.
[7] J.P. Vareda, A.J.M. Valente, L. Durães, Heavy metals in Iberian soils: Removal by current adsorbents/amendments and prospective for aerogels, Adv. Colloid Interface Sci. 237 (2016) 28–42, https://doi.org/10.1016/j.cis.2016.08.009.
[8] A.M. Alsuhaibani, A.A.A. Alayyafi, L.A. Albedair, M.G. El-Desouky, A.A. El-Bindary, Efficient fabrication of a composite sponge for Cr(VI) removal via citric acid cross-linking of metal-organic framework and chitosan: Adsorption isotherm, kinetic studies, and optimization using Box-Behnken design, Mater. Today Sustain. 26 (2024), https://doi.org/10.1016/j.mtsust.2024.100732.
[9] H.M. Nassef, G.A.A.M. Al-Hazmi, A.A.A. Alayyafi, M.G. El-Desouky, A.A. El-Bindary, Synthesis and characterization of new composite sponge combining of metal-organic framework and chitosan for the elimination of Pb(II), Cu(II) and Cd (II) ions from aqueous solutions: Batch adsorption and optimization using Box-Behnken design, J. Mol. Liq. 394 (2024) 123741, https://doi.org/10.1016/j.molliq.2023.123741.
[10] L. Monser, N. Adhoum, Modified activated carbon for the removal of copper, zinc, chromium and cyanide from wastewater, Sep. Purif. Technol. 26 (2002) 137–146, https://doi.org/10.1016/S1383-5866(01)00155-1.
[11] A.C. Boccia, M. Neagu, A. Pulvirenti, Bio-Based Aerogels for the Removal of Heavy Metal Ions and Oils from Water: Novel Solutions for Environmental Remediation, Gels. 10 (2024) 1–21, https://doi.org/10.3390/gels10010032.
[12] H. Maleki, Recent advances in aerogels for environmental remediation applications: A review, Chem. Eng. J. 300 (2016) 98–118, https://doi.org/10.1016/j.cej.2016.04.098.
[13] A. Milicevic, G. Branica, N. Raos, Irving-williams order in the framework of connectivity index 3xv enables simultaneous prediction of stability constants of bivalent transition metal complexes, Molecules. 16 (2011) 1103–1112, https://doi.org/10.3390/molecules16021103.
[14] L. Durães, H. Maleki, J.P. Vareda, A. Lamy-Mendes, A. Portugal, Exploring the versatile surface chemistry of silica aerogels for multipurpose application, MRS Adv. 2 (2017) 3511–3519, https://doi.org/10.1557/adv.2017.375.
[15] R.P. Dhavale, V.G. Parale, H. Choi, T. Kim, K.Y. Lee, V.D. Phadtare, H.H. Park, Epoxy-thiol crosslinking for enhanced mechanical strength in silica aerogels and highly efficient dye adsorption, Appl. Surf. Sci. 642 (2024) 158619, https://doi.org/10.1016/j.apsusc.2023.158619.
[16] P. Hedera, Wilson's disease: A master of disguise, Park. Relat. Disord. 59 (2019) 140–145, https://doi.org/10.1016/j.parkreldis.2019.02.016.
[17] S. Štandeker, A. Veronovski, Z. Novak, Ž. Knez, Silica aerogels modified with mercapto functional groups used for Cu(II) and Hg(II) removal from aqueous solutions, Desalination. 269 (2011) 223–230, https://doi.org/10.1016/j.desal.2010.10.064.
[18] H.R. Pouretedal, M. Kazemi, Characterization of modified silica aerogel using sodium silicate precursor and its application as adsorbent of Cu2+, Cd2+, and Pb2 + ions, Int. J. Ind. Chem. 3 (2012) 1–8, https://doi.org/10.1186/2228-5547-3-20.
[19] V.G. Parale, H. Choi, T. Kim, V.D. Phadtare, R.P. Dhavale, K.Y. Lee, A. Panda, H. H. Park, One pot synthesis of hybrid silica aerogels with improved mechanical properties and heavy metal adsorption: Synergistic effect of in situ epoxy-thiol polymerization and sol-gel process, Sep. Purif. Technol. 308 (2023) 122934, https://doi.org/10.1016/j.seppur.2022.122934.
[20] H. Choi, H.H. Han, V.G. Parale, T. Kim, W. Park, Y. Kim, J. Kim, Y. Choi, Y.S. Bae, H.H. Park, Rigid amine-incorporated silica aerogel for highly efficient CO2 capture and heavy metal removal, Chem. Eng. J. 483 (2024) 149357, https://doi.org/10.1016/j.cej.2024.149357.
[21] X. Duan, G. Qi, P. Wang, E.P. Giannelis, A highly efficient and selective polysilsesquioxane sorbent for heavy metal removal, ChemPhysChem. 13 (2012) 2536–2539, https://doi.org/10.1002/cphc.201100988.
[22] J.P. Vareda, L. Durães, Functionalized silica xerogels for adsorption of heavy metals from groundwater and soils, J. Sol-Gel Sci. Technol. 84 (2017) 400–408, https://doi.org/10.1007/s10971-017-4326-y.
[23] J.P. Vareda, A.J.M. Valente, L. Durães, Assessment of heavy metal pollution from anthropogenic activities and remediation strategies: A review, J. Environ. Manage. 246 (2019) 101–118, https://doi.org/10.1016/j.jenvman.2019.05.126.
[24] J. Han, Z. Du, W. Zou, H. Li, C. Zhang, Fabrication of interfacial functionalized porous polymer monolith and its adsorption properties of copper ions, J. Hazard. Mater. 276 (2014) 225–231, https://doi.org/10.1016/j.jhazmat.2014.05.035.
[25] P. Wojciechowska, R. Cierpiszewski, H. Maciejewski, Gelatin–Siloxane Hybrid Monoliths as Novel Heavy Metal Adsorbents, Appl. Sci. 12 (2022), https://doi.org/10.3390/app12031258.
[26] Y. Wang, K. Cui, J. Bai, B. Fang, F. Wang, Cost-Effective Preparation of Gold Tailing-Based Aerogels for Efficient Adsorption of Copper Ions from Wastewater, Water (switzerland). 15 (2023), https://doi.org/10.3390/w15040669.
[27] Commission Implementing Regulation (EU) 2018/1039, 2018.
[28] S. Alasti Bonab, J. Moghaddas, M. Rezaei, In-situ synthesis of silica aerogel/polyurethane inorganic-organic hybrid nanocomposite foams: Characterization, cell microstructure and mechanical properties, Polymer (guildf). 172 (2019) 27–40, https://doi.org/10.1016/j.polymer.2019.03.050.
[29] P. Cimavilla-Román, S. Pérez-Tamarit, M. Santiago-Calvo, M.Á. Rodríguez-Pérez, Influence of silica aerogel particles on the foaming process and cellular structure of

rigid polyurethane foams, Eur. Polym. J. 135 (2020) 109884, https://doi.org/10.1016/j.eurpolymj.2020.109884.
[30] M. Santiago-Calvo, J. Tirado-Mediavilla, J.L. Ruiz-Herrero, M.Á. Rodríguez-Pérez, F. Villafañe, The effects of functional nanofillers on the reaction kinetics, microstructure, thermal and mechanical properties of water blown rigid polyurethane foams, Polymer (guildf). 150 (2018) 138–149, https://doi.org/10.1016/j.polymer.2018.07.029.
[31] Z. Talebi Mazraeh-shahi, A. Mousavi Shoushtari, A.R. Bahramian, M. Abdouss, Synthesis, pore structure and properties of polyurethane/silica hybrid aerogels dried at ambient pressure, J. Ind. Eng. Chem. 21 (2015) 797–804, https://doi.org/10.1016/j.jiec.2014.04.015.
[32] B. Merillas, A. Lamy-Mendes, F. Villafañe, L. Durães, M.Á. Rodríguez-Pérez, Polyurethane foam scaffold for silica aerogels : effect of cell size on the mechanical properties and thermal insulation, Mater. Today Chem. 26 (2022) 101257, https://doi.org/10.1016/j.mtchem.2022.101257.
[33] B. Merillas, A. Lamy-Mendes, F. Villafañe, L. Durães, M.Á. Rodríguez-Pérez, Silica-based aerogel composites reinforced with reticulated polyurethane foams: thermal and mechanical properties, Gels. 8 (2022) 392, https://doi.org/10.3390/gels8070392.
[34] ASTM D1622-08: Standard Test Method for Apparent Density of Rigid Cellular Plastics, ASTM International, West Conshohocken, PA, USA, 2008. doi:10.1520/D1622-20.
[35] P. Cimavilla-Román, M. Santiago-Calvo, M.Á. Rodríguez-Pérez, Dynamic Mechanical Analysis during polyurethane foaming: Relationship between modulus build-up and reaction kinetics, Polym. Test. 103 (2021), https://doi.org/10.1016/j.polymertesting.2021.107336.
[36] L. Juhász, K. Moldován, P. Gurikov, F. Liebner, I. Fábián, J. Kalmár, C. Cserháti, False morphology of aerogels caused by gold coating for sem imaging, Polymers (basel). 13 (2021) 1–12, https://doi.org/10.3390/polym13040588.
[37] E.P. Barrett, L.G. Joyner, P.P. Halenda, The Determination of Pore Volume and Area Distributions in Porous Substances. I. Computations from Nitrogen Isotherms, J. Am. Chem. Soc. 73 (1951) 373–380, https://doi.org/10.1021/ja01145a126.
[38] J. Pinto, E. Solórzano, M.A. Rodriguez-Perez, J.A. de Saja, Characterization of the cellular structure based on user-interactive image analysis procedures, J. Cell. Plast. 49 (2013) 555–575, https://doi.org/10.1177/0021955X13503847.
[39] Standard Test Method for Corona-Treated Polymer Films Using Water Contact Angle Measurements - ASTM D5946-17, 2017. doi:10.1520/D5946-09.10.1520/D5946-17.2.
[40] J.P. Vareda, L. Durães, Efficient adsorption of multiple heavy metals with tailored silica aerogel-like materials, Environ. Technol. 40 (2017) 529–541, https://doi.org/10.1080/09593330.2017.1397766.
[41] A. Lamy-Mendes, R.B. Torres, J.P. Vareda, D. Lopes, M. Ferreira, V. Valente, A. V. Girão, A.J.M. Valente, L. Durães, Amine modification of silica aerogels/xerogels for removal of relevant environmental pollutants, Molecules. 24 (2019) 10–14, https://doi.org/10.3390/molecules24203701.
[42] Y. Wei, T. Chen, Z. Qiu, H. Liu, Y. Xia, Z. Wang, R. Zou, C. Liu, Enhanced lead and copper removal in wastewater by adsorption onto magnesium oxide homogeneously embedded hierarchical porous biochar, Bioresour. Technol. 365 (2022), https://doi.org/10.1016/j.biortech.2022.128146.
[43] I. Langmuir, The constitution and fundamental properties of solids and liquids. Part II.-Liquids, J. Franklin Inst. 184 (1917) 721, https://doi.org/10.1016/s0016-0032(17)90088-2.
[44] H.M.F. Freundlich, Over the Adsorption in Solution, J. Phys. Chem. 57 (1906) 385–471.
[45] R. Sips, The Structure of a Catalyst Surface, J. Chem. Phys. 16 (1948) 490–495.
[46] S. Azizian, S. Eris, Adsorption isotherms and kinetics, first ed., Elsevier Ltd., 2021. doi:10.1016/B978-0-12-818805-7.00011-4.
[47] K.S.W. Sing, D.H. Everett, R.A.W. Haul, L. Moscou, R.A. Pierotti, J. Rouquerol, T. Siemieniewska, Reporting Physisorption Data for Gas/Solid Systems with Special Reference to the Determination of Surface Area and Porosity, Int. Union Pure Appl. Chem. 57 (1985) 603–619, https://doi.org/10.1351/pac198557040603.
[48] D. Posada, T.R. Buckley, Model selection and model averaging in phylogenetics: Advantages of akaike information criterion and bayesian approaches over likelihood ratio tests, Syst. Biol. 53 (2004) 793–808, https://doi.org/10.1080/10635150490522304.
[49] C. Jiao, J. Xiong, J. Tao, S. Xu, D. Zhang, H. Lin, Y. Chen, Sodium alginate/graphene oxide aerogel with enhanced strength-toughness and its heavy metal adsorption study, Int. J. Biol. Macromol. 83 (2016) 133–141, https://doi.org/10.1016/j.ijbiomac.2015.11.061.
[50] J.P. Vareda, A.J.M. Valente, L. Durães, Silica aerogels/xerogels modified with nitrogen-containing groups for heavy metal adsorption, Molecules. 25 (2020) 15–19, https://doi.org/10.3390/molecules25122788.
[51] H. Faghihian, H. Nourmoradi, M. Shokouhi, Removal of copper (II) and nickel (II) from aqueous media using silica aerogel modified with amino propyl triethoxysilane as an adsorbent: Equilibrium, kinetic, and isotherms study, Desalin. Water Treat. 52 (2014) 305–313, https://doi.org/10.1080/19443994.2013.785367.
[52] T. Chaisuwan, T. Komalwanich, S. Luangsukrerk, S. Wongkasemjit, Removal of heavy metals from model wastewater by using polybenzoxazine aerogel, Desalination. 256 (2010) 108–114, https://doi.org/10.1016/j.desal.2010.02.005.
[53] A. Lamy-Mendes, R.B. Torres, J.P. Vareda, D. Lopes, M. Ferreira, V. Valente, A. V. Girão, A.J.M. Valente, L. Durães, Amine modification of silica aerogels/xerogels for removal of relevant environmental pollutants, Molecules. 24 (2019) 3701, https://doi.org/10.3390/molecules24203701.
[54] E.G. Deze, S.K. Papageorgiou, E.P. Favvas, F.K. Katsaros, Porous alginate aerogel beads for effective and rapid heavy metal sorption from aqueous solutions: Effect of porosity in Cu2+ and Cd2+ ion sorption, Chem. Eng. J. 209 (2012) 537–546, https://doi.org/10.1016/j.cej.2012.07.133.
[55] J.P. Vareda, P.M.C. Matias, J.A. Paixão, D. Murtinho, A.J.M. Valente, L. Durães, Chitosan–silica composite aerogel for the adsorption of cupric ions, Gels. 10 (2024), https://doi.org/10.3390/gels10030192.
[56] S. Lagergreen, Zur Theorie der sogenannten Adsorption gelöster Stoffe, Zeitschrift Für Chemie Und Ind, Der Kolloide. 2 (1907) 15, https://doi.org/10.1007/bf01501332.
[57] Y.S. Ho, G. McKay, Sorption of dye from aqueous solution by peat, Chem. Eng. J. 70 (1998) 115–124, https://doi.org/10.1016/S1385-8947(98)00076-X.
[58] N. Chiron, R. Guilet, E. Deydier, Adsorption of Cu(II) and Pb(II) onto a grafted silica: Isotherms and kinetic models, Water Res. 37 (2003) 3079–3086, https://doi.org/10.1016/S0043-1354(03)00156-8.
[59] S.Y. Elovich, O.G. Larinov, Theory of Adsorption from Solutions of Non Electrolytes on Solid (I) Equation Adsorption from Solutions and the Analysis of Its Simplest Form, (II) Verification of the Equation of Adsorption Isotherm from Solutions, Izv. Akad. Nauk. SSSR, Otd. Khimicheskikh Nauk. 2 (1962) 209–219.
[60] A. Alfarra, E. Frackowiak, F. Béguin, The HSAB concept as a means to interpret the adsorption of metal ions onto activated carbons, Appl. Surf. Sci. 228 (2004) 84–92, https://doi.org/10.1016/j.apsusc.2003.12.033.
[61] R. Ezzati, Derivation of Pseudo-First-Order, Pseudo-Second-Order and Modified Pseudo-First-Order rate equations from Langmuir and Freundlich isotherms for adsorption, Chem. Eng. J. 392 (2020) 123705, https://doi.org/10.1016/j.cej.2019.123705.
[62] A.J.M. Valente, D. Pirozzi, A. Cinquegrana, G. Utzeri, D. Murtinho, F. Sannino, Synthesis of β-cyclodextrin-based nanosponges for remediation of 2,4-D polluted waters, Environ. Res. 215 (2022), https://doi.org/10.1016/j.envres.2022.114214.